

Isoelectronic perturbations to f - d -electron hybridization and the enhancement of hidden order in URu₂Si₂

C. T. Wolowiec,^{1,2} N. Kanchanavatee,³ K. Huang,⁴ S. Ran,⁵ A. J. Breindel,^{1,2} N. Pouse,¹ Kalyan Sasmal,^{1,2} R. E. Baumbach,^{6,7} G. Chappell,^{6,7} Peter S. Riseborough,⁸ and M. B. Maple^{1,2,*}

¹Department of Physics, University of California, San Diego, La Jolla, California 92093, USA

²Center for Advanced Nanoscience, University of California, San Diego, La Jolla, California 92093, USA

³Department of Physics, Chulalongkorn University, Pathumwan 10330, Thailand

⁴Lawrence Livermore National Laboratory, Livermore, California 94550, USA

⁵Department of Physics, Washington University in St. Louis, St. Louis, Missouri 63130, USA

⁶National High Magnetic Field Laboratory, Florida State University, Tallahassee, Florida 32310, USA

⁷Department of Physics, Florida State University, Tallahassee, Florida 32306, USA

⁸Physics Department, Temple University, Philadelphia, PA 19122, USA

(Dated: September 25, 2020)

Electrical resistivity measurements were performed on single crystals of URu_{2-x}Os_xSi₂ up to $x = 0.28$ under hydrostatic pressure up to $P = 2$ GPa. As the Os concentration, x , is increased, (1) the lattice expands, creating an effective *negative* chemical pressure $P_{ch}(x)$, (2) the hidden order (HO) phase is enhanced and the system is driven toward a large-moment antiferromagnetic (LMAFM) phase, and (3) less external pressure P_c is required to induce the HO→LMAFM phase transition. We compare the $T(x, P)$ phase behavior reported here for the URu_{2-x}Os_xSi₂ system with previous reports of enhanced HO in URu₂Si₂ upon tuning with P , or similarly in URu_{2-x}Fe_xSi₂ upon tuning with *positive* $P_{ch}(x)$. It is noted that pressure, Fe substitution, and Os substitution are the only known perturbations that enhance the HO phase and induce the first order transition to the LMAFM phase in URu₂Si₂. We present a scenario in which the application of pressure or the isoelectronic substitution of Fe and Os ions for Ru results in an increase in the hybridization of the U-5*f*- and transition metal *d*-electron states which leads to electronic instability in the paramagnetic phase and a concurrent stability of HO (and LMAFM) in URu₂Si₂. Calculations in the tight binding approximation are included to determine the strength of hybridization between the U-5*f* electrons and each of the isoelectronic transition metal *d*-electron states of Fe, Ru, and Os.

PACS numbers: 71.27.+a, 72.10.Di, 74.62.Dh, 74.62.Fj

I. INTRODUCTION

The heavy-fermion superconducting compound URu₂Si₂ is known for its second-order phase transition into the so-called “hidden order” (HO) phase at a transition temperature $T_0 \approx 17.5$ K. Extensive investigation of the phase space in proximity to the HO phase transition has provided a detailed picture of the electronic and magnetic structure of this unique phase.^{1–42} However, more than three decades after the initial characterization of URu₂Si₂,^{1–3} the order parameter for the HO phase is still unidentified.

Most perturbations to the URu₂Si₂ compound have the effect of suppressing HO. The application of an external magnetic field (H) suppresses the HO phase^{41,43} and many of the chemical substitutions (x) at the U, Ru, or Si sites that have been explored, significantly reduce T_0 , even at modest levels of substituent concentration.^{44–52} At present, only three perturbations are known to consistently *enhance* the HO phase in URu₂Si₂: (1) external pressure P , (2) isoelectronic substitution of Fe ions for Ru, and (3) isoelectronic substitution of Os ions for Ru. Upon applying pressure P , the HO phase in pure URu₂Si₂ is enhanced⁶ and the system is driven toward a

large moment antiferromagnetic (LMAFM) phase.⁵³ The HO→LMAFM phase transition is identified indirectly by a characteristic “kink” at a critical pressure $P_c \approx 1.5$ GPa in the $T_0(P)$ phase boundary,^{18,53,54} and also directly by neutron diffraction experiments, which reveal an increase in the magnetic moment from $\mu \sim (0.03 \pm 0.02)\mu_B/U$ in the HO phase to $\mu \sim 0.4 \mu_B/U$ in the LMAFM phase.^{13,55,56}

Recent reports indicate that the isoelectronic substitution of Fe ions for Ru in URu₂Si₂ replicates the $T_0(P)$ behavior in URu₂Si₂.^{57–59} An increase in x in URu_{2-x}Fe_xSi₂ enhances the HO phase and drives the system toward the HO→LMAFM phase transition at a critical Fe concentration $x_c \approx 0.15$.^{58,60} The decrease in the volume of the unit cell due to substitution of smaller Fe ions for Ru may be interpreted as a chemical pressure, P_{ch} , where the Fe concentration x can be converted to $P_{ch}(x)$.^{57,59} In addition, the induced HO→LMAFM phase transition in URu_{2-x}Fe_xSi₂ occurs at combinations of x and P that consistently obey the additive relationship: $P_{ch}(x) + P_c \approx 1.5$ GPa.^{57,59} These results have led to the suggestion that P_{ch} is equivalent to P in affecting the HO and LMAFM phases.^{58,59}

Reports of the isoelectronic substitution of larger Os ions for Ru have shown that an increase in x in URu_{2-x}Os_xSi₂: (1) expands the volume of the unit cell, thus creating an effective *negative* chemical pressure ($P_{ch} \leq 0$), (2) enhances the HO phase, and (3) drives the

* Corresponding Author: mbmaple@ucsd.edu

system toward a similar HO→LMAFM phase transition at a critical Os concentration of $x_c \approx 0.065$.^{60–62} These results are contrary to the expectation that a *negative* P_{ch} would lead to a suppression of HO and complicates the view of “chemical pressure” as a mechanism affecting the evolution of phases in URu_2Si_2 .

In this paper, we report on the $T(x, P)$ phase behavior for the $\text{URu}_{2-x}\text{Os}_x\text{Si}_2$ system based on $\rho(T)$ measurements of single crystals of $\text{URu}_{2-x}\text{Os}_x\text{Si}_2$ as a function of Os concentration x , and applied pressure P . The $T(x, P)$ phase behavior observed here for the $\text{URu}_{2-x}\text{Os}_x\text{Si}_2$ system^{57–59} is compared to that of the $\text{URu}_{2-x}\text{Fe}_x\text{Si}_2$ system and also with the $T(P)$ behavior in pure URu_2Si_2 . As an explanation for the enhancement of HO toward the HO→LMAFM phase transition, we suggest a scenario in which each of the perturbations of Os substitution, Fe substitution, and pressure P favors delocalization of the $5f$ electrons and increases the hybridization of the uranium $5f$ - and transition metal (Fe, Ru, Os) d -electron states. In order to avoid an ad-hoc explanation of the effect of increasing the Os concentration x in $\text{URu}_{2-x}\text{Os}_x\text{Si}_2$, compared to the effects of pressure P and Fe substitution, we explain how pressure P , Fe substitution, and Os substitution are three perturbative routes to enhancement of the U- $5f$ - and d -electron hybridization. The importance of the $5f$ - and d -electron hybridization to the emergence of HO/LMAFM is presented in the context of the Fermi surface instability that leads to a reconstruction and partial gapping of the Fermi-surface during the transition from the paramagnetic (PM) phase to the HO and LMAFM phases.^{2,6,20,22,24–26,37,38,63}

In an effort to further understand the effect of isoelectronic substitution on the $5f$ - and d -electron hybridization, calculations in the tight-binding approximation were made for compounds from the series UM_2Si_2 ($M = \text{Fe, Ru, and Os}$). The calculations indicate that the degree of hybridization is largely dependent on the magnitude of the difference between the binding energy of the localized U- $5f$ electrons and that of the transition metal d electrons.

II. EXPERIMENTAL DETAILS

The experimental design and procedure, including synthesis of single crystals, crystallographic measurements, and measurements of electrical resistivity under applied pressure are similar to those in the investigation of the $\text{URu}_{2-x}\text{Fe}_x\text{Si}_2$ system as described in Ref. 59. Single crystals of $\text{URu}_{2-x}\text{Os}_x\text{Si}_2$ at nominal concentrations of $x_{nom} = 0, 0.025, 0.05, 0.10, 0.13, 0.16, \text{ and } 0.20$ were grown according to the Czochralski method in a tetra-Arc furnace. The quality of the single crystal samples were determined by Laue X-ray diffraction patterns together with X-ray powder diffraction (XRD) measurements. The XRD patterns were fitted according to the Rietveld refinement technique using the *GSAS-II* software package.⁶⁴ Elemental analysis of single crystal sam-

ples of $\text{URu}_{2-x}\text{Os}_x\text{Si}_2$ at nominal concentrations of $x_{nom} = 0.025, 0.05, 0.10, 0.13, \text{ and } 0.20$ was performed using energy-dispersive X-ray spectroscopy (EDX). Based on the EDX measurements, the actual osmium concentrations x_{act} in these samples were determined to be $x_{act} = 0.07, 0.08, 0.15, 0.18, \text{ and } 0.28$, respectively. In this report, the Os concentration x in these single crystal $\text{URu}_{2-x}\text{Os}_x\text{Si}_2$ samples is taken as x_{act} as determined from the EDX measurements, unless otherwise stated. It is noted that the single crystal sample with nominal Os concentration $x_{nom} = 0.16$ was not available for EDX measurement and thus $x = x_{nom} = 0.16$ in this case. (See Sec. VI for details on sample quality and the error in Os concentration.)

Annealed Pt wire leads were affixed with silver epoxy to gold-sputtered contact surfaces on each sample in a standard four-wire configuration. Electrical resistivity $\rho(T)$ measurements were performed on single crystals of $\text{URu}_{2-x}\text{Os}_x\text{Si}_2$ under applied pressure up to $P = 2$ GPa for Os concentrations $x = 0, 0.07, 0.08, 0.15, 0.16, 0.18$ and 0.28 . A 1:1 mixture by volume of n -pentane and isoamyl alcohol was used to provide a quasi-hydrostatic pressure transmitting medium and the pressure was locked in with the use of a beryllium copper clamped piston-cylinder pressure cell. The pressure dependence of the superconducting transition temperature of high purity Sn was used as a manometer. Measurements of $\rho(T)$ were performed upon warming from ~ 1 to 300 K in a pumped ^4He dewar and the temperature was determined from the four-wire electrical resistivity of a calibrated Cernox sensor.

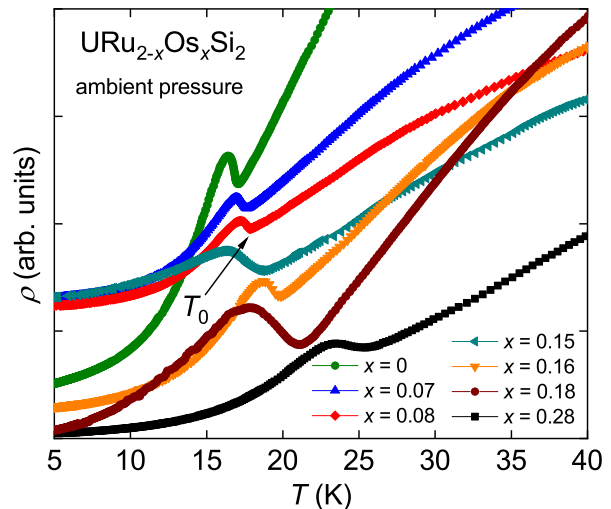


FIG. 1. (Color online) Electrical resistivity $\rho(T)$ in the vicinity of the HO/LMAFM transition for the $\text{URu}_{2-x}\text{Os}_x\text{Si}_2$ system at ambient pressure for $x = 0, 0.07, 0.08, 0.15, 0.16, 0.18, \text{ and } 0.28$. The transition temperature T_0 is indicated by the black arrow. The $\rho(T)$ curves have been shifted vertically for clarity.

III. RESULTS

Figure 1 displays the temperature dependence of the ambient pressure electrical resistivity $\rho(T)$ in the vicinity of the transition temperature T_0 for the $\text{URu}_{2-x}\text{Os}_x\text{Si}_2$ system. The transition from the paramagnetic (PM) phase to the HO phase (or LMAFM phase at higher values of x) is defined to be at the location of the minimum in $\rho(T)$, which occurs prior to the upturn in $\rho(T)$ upon cooling, as indicated by the black arrow. It is clear that the feature in $\rho(T)$ shifts to higher temperature as x is increased.

The values of T_0 , as determined from the $\rho(T)$ data shown in Fig. 1 for single crystal samples of $\text{URu}_{2-x}\text{Os}_x\text{Si}_2$ at $x = 0, 0.07, 0.08, 0.15, 0.16, 0.18,$ and 0.28 , were used to construct the T - x phase diagram displayed in Fig. 2. The solid black lines that outline the $T_0(x)$ phase boundary between the PM phase and the HO (or LMAFM) phase are linear fits to the $T_0(x)$ data. The solid black line of smaller slope outlining the $T_0(x)$ phase boundary between the PM phase and the HO phase is a linear fit to the $T_0(x)$ data for samples with low Os concentrations up to $x = 0.15$. The solid black line of larger slope outlining the $T_0(x)$ phase boundary between the PM phase and the LMAFM phase is a linear fit to the $T_0(x)$ data for the single crystal samples with Os concentrations from $x = 0.15$ to 0.28 . The intersection of the two lines forms a “kink” in the $T_0(x)$ phase boundary and is taken to be the location of the

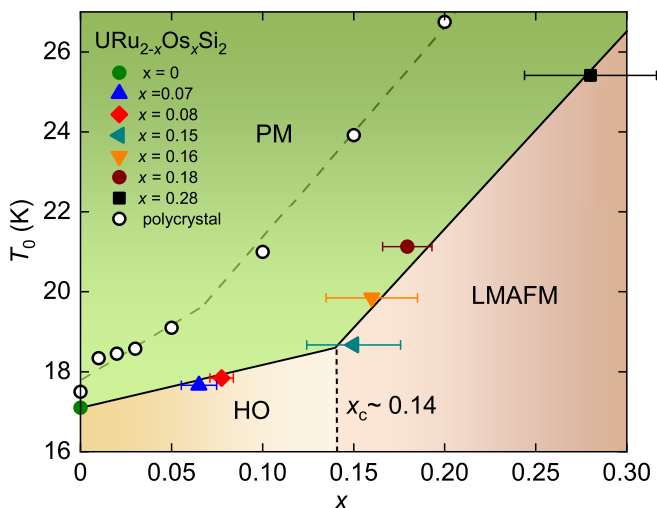


FIG. 2. (Color online) T_0 vs x phase diagram for $\text{URu}_{2-x}\text{Os}_x\text{Si}_2$ up to $x = 0.28$. The solid black and green dashed lines representing the $T_0(x)$ phase boundaries are linear fits to the values of T_0 for the single crystal and polycrystalline samples, respectively. The values of T_0 were determined from $\rho(T)$ data as shown in Fig. 1 (see text) and the values of T_0 for the polycrystalline samples (white circles) were similarly determined as reported in Ref. 61. The vertical dashed line locates the critical Os concentration $x_c \approx 0.14$ at the HO \rightarrow LMAFM phase transition. Error bars for x represent standard deviations in the data from EDX measurements (see Sec. VI).

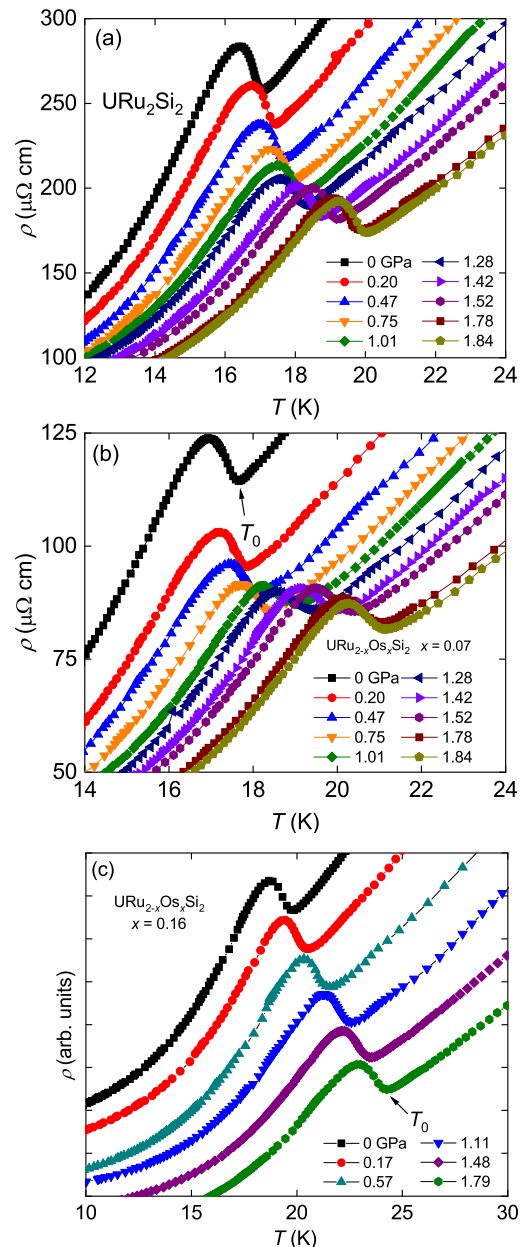


FIG. 3. (Color online) Electrical resistivity $\rho(T)$ in the vicinity of the HO/LMAFM transition for the $\text{URu}_{2-x}\text{Os}_x\text{Si}_2$ system as a function of pressure P : (a) $\rho(T)$ for pure URu_2Si_2 as a function of pressure up to $P = 1.9$ GPa; (b) $\rho(T)$ for the $x = 0.07$ sample as a function of pressure up to $P = 1.9$ GPa; and (c) $\rho(T)$ for the $x = 0.16$ sample as a function of pressure up to 1.8 GPa. The $\rho(T)$ data for $x = 0.16$ have been shifted vertically for clarity.

HO \rightarrow LMAFM transition at a critical Os concentration of $x_c \approx 0.14$.

Similar linear fits (dashed green lines) to the values of T_0 (white circles) taken from Ref. 61 for polycrystalline samples of $\text{URu}_{2-x}\text{Os}_x\text{Si}_2$ suggest a critical concentration of $x_c \approx 0.07$. Given the differences inherent to synthesis of polycrystals compared to single crystals, the discrepancy between the values of the critical concentra-

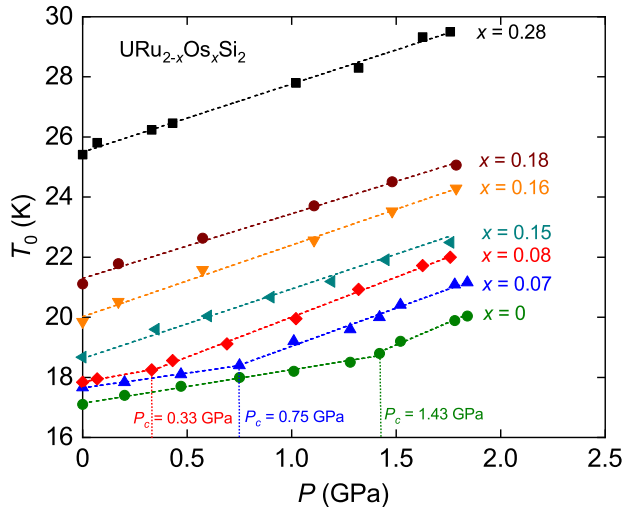


FIG. 4. (Color online) A “composite” T_0 vs P phase diagram for $\text{URu}_{2-x}\text{Os}_x\text{Si}_2$. The dashed lines representing the $T_0(P)$ phase boundary are linear fits to the $T_0(P)$ data. The values of the critical pressures $P_c = 1.43, 0.75, 0.33$ for $x = 0, 0.07, \text{ and } 0.08$, respectively, mark the pressure-induced HO \rightarrow LMAFM phase transition and are defined by the location of the “kinks” in the $T_0(P)$ phase boundaries (or intersections of the linear fits) (see text).

tion for the polycrystalline and single crystal samples is not clearly understood. However, the two $T_0(x)$ phase boundaries for polycrystalline and single crystal samples of $\text{URu}_{2-x}\text{Os}_x\text{Si}_2$ are qualitatively similar with the $T_0(x)$ phase boundary for single crystals being shifted toward higher Os concentration x .

Figure 3 displays the temperature dependence of the electrical resistivity $\rho(T)$ near T_0 for the $\text{URu}_{2-x}\text{Os}_x\text{Si}_2$ system under applied pressure P . Figure 3(a) displays $\rho(T)$ for pure URu_2Si_2 as a function of pressure up to $P \approx 1.9$ GPa. As pressure is increased, the feature in $\rho(T)$ shifts to higher temperature similar to what is observed with an increase in x . Furthermore, the feature in $\rho(T)$ appears to migrate more quickly with pressure above some critical pressure near 1.4 GPa. Figures 3(b) and (c) display $\rho(T)$ in the vicinity of T_0 as a function of applied pressure for samples at $x = 0.07$ and 0.16, respectively. The sample with $x = 0.07$ (Fig. 3(b)) is at an Os concentration well below the critical concentration $x_c \approx 0.14$ and therefore exhibits the HO phase up to some critical pressure. As with the pure compound URu_2Si_2 , the pressure dependence of the feature in $\rho(T)$ increases above some critical pressure P_c near 0.8 GPa. In contrast, for the sample with an Os concentration $x = 0.16$ (Fig. 3(c)) greater than x_c , the pressure dependence of the feature in $\rho(T)$ is constant up to 2 GPa suggesting the sample is likely already homogenous in the LMAFM phase at ambient pressure.

The $T_0(P)$ behavior for all seven single crystal samples from the $\text{URu}_{2-x}\text{Os}_x\text{Si}_2$ system (at $x = 0, 0.07, 0.08, 0.15, 0.16, 0.18, \text{ and } 0.28$) is plotted in the “composite” T_0 vs P phase diagram shown in Fig. 4. The $T_0(P)$ phase boundaries for samples with $x = 0, 0.07, \text{ and } 0.08$ exhibit the characteristic discontinuity or “kink”, which

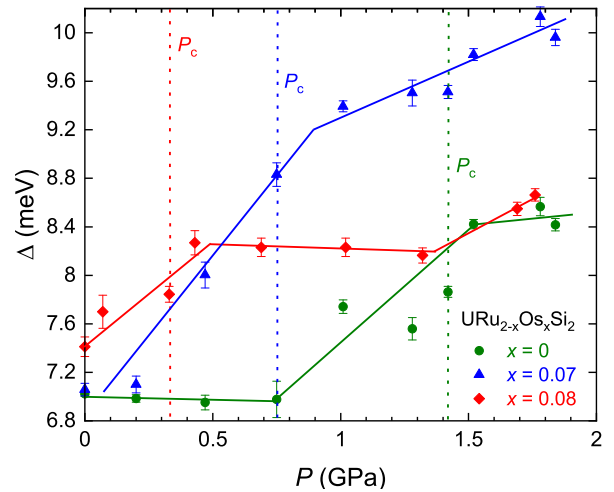


FIG. 5. (Color online) Energy gap Δ vs. pressure P for the $x = 0, 0.07, \text{ and } 0.08$ samples. The value of Δ are based on fits to the low temperature $\rho(T)$ data as explained in the text. The values of P_c (marked by dashed vertical lines) were determined from the “kinks” in the T_0 vs. P phase boundaries shown in Fig. 4. The error in Δ was determined by the fitting algorithm and the solid lines are guides to the eye.

is indicative of the first-order HO \rightarrow LMAFM phase transition. The slopes of the $T_0(P)$ phase boundaries in the HO phase, prior to the discontinuities, for the $x = 0, 0.07, \text{ and } 0.08$ samples are $dT_0/dP = 1.11, 0.99, \text{ and } 1.21$ K GPa^{-1} , respectively. In the LMAFM phase, the slopes are significantly higher at $dT_0/dP = 2.99, 2.53, \text{ and } 2.66$ K GPa^{-1} , respectively. There is no discontinuity in the slope of the $T_0(P)$ phase boundaries for the Os-substituted samples with higher Os concentrations of $x = 0.15, 0.16, 0.18, \text{ and } 0.28$ that are above x_c , where the slopes were determined to be $dT_0/dP = 2.31, 2.42, 2.15 \text{ and } 2.27$ K GPa^{-1} , respectively. Note the equivalence between the values of the pressure dependence in both the HO phase (averaged at $dT_0/dP \approx 1.10$ K GPa^{-1}) and the LMAFM phase (averaged at $dT_0/dP = 2.47$ K GPa^{-1}) across all of the samples. The values of all slopes were determined by linear fits (solid lines in Fig. 4) to the $T_0(P)$ data in the HO or LMAFM phases and are in very good agreement with hydrostatic pressure coefficients reported in other investigations.^{18,53,59,65}

The pressure dependence of the charge gap Δ that opens up over the Fermi surface during its reconstruction at the PM \rightarrow HO/LMAFM phase transition may serve as another measure of the critical pressure P_c . Namely, the critical pressure P_c can be taken as the value of P where there is a change in the pressure dependence of Δ that occurs at the first-order phase transition from HO to LMAFM. Figure 5 displays a plot of the energy gap Δ as a function of pressure P for single crystal samples of $\text{URu}_{2-x}\text{Os}_x\text{Si}_2$ with $x = 0, 0.07, 0.08$. The values of Δ were extracted from fits of a theoretical model⁶⁶ of electrical resistivity to the $\rho(T)$ data in the low temperature region below the feature in electrical

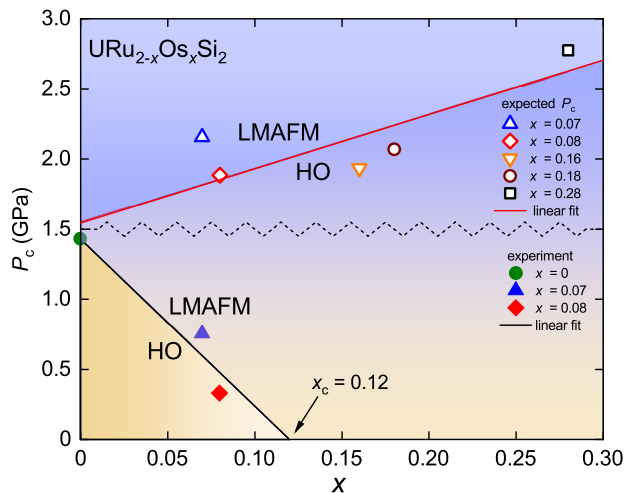


FIG. 6. (Color online) Measured and expected critical pressure P_c as a function of x for $\text{URu}_{2-x}\text{Os}_x\text{Si}_2$. As x is increased, the critical pressure is reduced to $P_c = 0$ GPa at a critical Os concentration of $x_c \sim 0.12$. The open symbols represent the expected critical pressure P_c (see text). The black (red) solid lines represent the experimental (expected) HO/LMAFM phase boundaries and are linear fits to the experimental (expected) values of critical pressure P_c .

resistivity (where $d\rho/dT > 0$) as described in Ref. 59. From the Δ vs. P plots for each of the $x = 0, 0.07, 0.08$ samples, there is a flattening of the pressure coefficient $d\Delta/dP$ at pressures of $P \approx 1.55, 0.90,$ and 0.50 GPa that are consistent with the critical pressures $P_c = 1.43, 0.75, 0.33$ GPa determined from the $T_0(P)$ phase boundaries in Fig. 4. Interestingly, the “kinks” in Δ vs. P data occur at pressures that are consistently ~ 0.15 GPa higher than the P_c values. Low values of $\Delta \approx 7.2$ meV correspond to transitions into the HO phase. Higher values of $\Delta > 8.5$ meV correspond to transitions into the LMAFM phase. Intermediate values of Δ preceding the plateau in the $\Delta(P)$ curves suggest inhomogeneity and a percolation of the LMAFM phase as pressure is increased.

Of central importance to the current report is the reduction of the critical pressure P_c with increasing Os concentration x , as illustrated in Fig. 4. The vertical dashed lines locate decreasing values of $P_c = 1.43, 0.75,$ and 0.33 GPa for samples in order of increasing Os concentration $x = 0, 0.07,$ and 0.08 . This is reminiscent of the reduction of P_c with increasing Fe concentration for the $\text{URu}_{2-x}\text{Fe}_x\text{Si}_2$ system.⁵⁹ Based on the results of the Fe-substituted system, in which lower values of P_c were required to induce the HO \rightarrow LMAFM transition according to the additive relation: $P_{ch}(x) + P_c \approx 1.5$ GPa, one would expect that *higher* (rather than lower) values of P_c are required to induce the HO \rightarrow LMAFM transition for Os-substituted URu_2Si_2 , which is biased with an effective *negative* chemical pressure ($P_{ch}(x) < 0$). However, this is not what we observed. The discrepancy between the expected increase in P_c and the reduction in P_c that was observed experimentally, is illustrated in the plot of P_c vs. x as shown in Fig. 6. The

solid black line with a negative slope is a linear fit to the experimentally determined values of P_c (filled symbols) and represents the $P_c(x)$ phase boundary between the HO and LMAFM phases for the $\text{URu}_{2-x}\text{Os}_x\text{Si}_2$ system. The extrapolation of the fit to zero pressure yields a critical Os concentration of $x = 0.12$, which is comparable to the value of $x_c = 0.14$ determined from the “kink” in T_0 vs x phase diagram displayed in Fig. 2. The open symbols in Fig. 6 represent the expected values of critical pressure P_c , which were determined by first converting the Os concentration x to a *negative* chemical pressure $P_{ch}(x)$ and then using the additive property of chemical and applied pressure: $P_{ch}(x) + P_c \approx 1.5$ GPa. The solid red line with positive slope is a linear fit to these expected values of P_c and represents the expected $P_c(x)$ phase boundary between the HO and LMAFM phases for the $\text{URu}_{2-x}\text{Os}_x\text{Si}_2$ system.

Other than pure URu_2Si_2 , Fe-substituted URu_2Si_2 , and Os-substituted URu_2Si_2 , the only known URu_2Si_2 -based system measured under pressure is Re-substituted URu_2Si_2 .¹⁸ At ambient pressure, the effect of Re substitution is to rapidly suppress HO toward an emergent itinerant ferromagnetic phase. Interestingly, as pressure is applied to samples from the $\text{URu}_{2-x}\text{Re}_x\text{Si}_2$ system, the HO phase is enhanced toward the same HO \rightarrow LMAFM phase transition. However, as the Re concentration is increased in $\text{URu}_{2-x}\text{Re}_x\text{Si}_2$ under pressure, the “kink” in the T_0 vs. P “composite” phase diagram persists at a critical pressure of $P_c = 1.5$ GPa. This difference is emphasized in Fig. 7 which displays T_0 - P - x phase diagrams for each of the $\text{URu}_{2-x}\text{Os}_x\text{Si}_2$, $\text{URu}_{2-x}\text{Fe}_x\text{Si}_2$ and $\text{URu}_{2-x}\text{Re}_x\text{Si}_2$ systems. The $T_0(x, P)$ data for the $\text{URu}_{2-x}\text{Re}_x\text{Si}_2$ system was taken from Ref. 18. (Due to the fact that the HO transition temperature T_0 is suppressed with increasing Re concentration, the values along the concentration (x) axis in Fig. 7(c) have been reversed for clarity.) Note the difference in the HO/LMAFM phase boundary in the x - P plane for the Re-substituted system in Fig. 7(c). The HO/LMAFM phase boundary is constant at $P_c = 1.5$ GPa for all Re concentrations up to $x = 0.08$ in $\text{URu}_{2-x}\text{Re}_x\text{Si}_2$, while the boundary is suppressed to $P = 0$ GPa as x is increased in the $\text{URu}_{2-x}\text{Fe}_x\text{Si}_2$ and $\text{URu}_{2-x}\text{Os}_x\text{Si}_2$ systems.

IV. DISCUSSION

Investigations of URu_2Si_2 under applied uniaxial and/or hydrostatic pressure show that an increase in pressure enhances HO (with an increase in T_0) and drives the system toward a pressure-induced antiferromagnetic phase (LMAFM) at a critical pressure of $P_c \approx 1.5$ GPa at the bicritical point (or at $P_x \approx 0.5$ GPa as $T \rightarrow 0$).^{13,18,53,65,67-72} Recently, a related investigation of Fe-substituted URu_2Si_2 under applied pressure established a quantitative equivalence between *positive* chemical pressure $P_{ch}(x)$ to external pressure P in affecting the phase

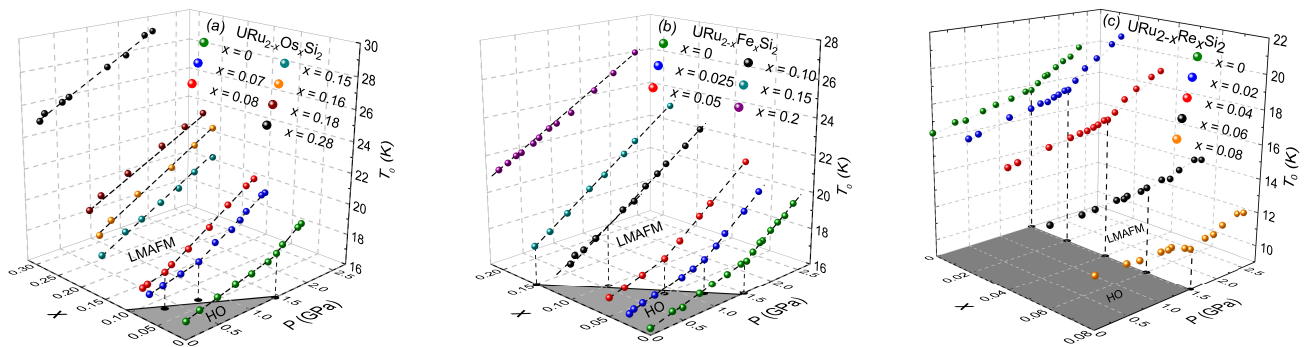


FIG. 7. (Color online) T_0 - P - x phase diagrams for the (a) $\text{URu}_{2-x}\text{Os}_x\text{Si}_2$ (b) $\text{URu}_{2-x}\text{Fe}_x\text{Si}_2$ and (c) $\text{URu}_{2-x}\text{Re}_x\text{Si}_2$ systems. The values along the concentration (x) axis for the $\text{URu}_{2-x}\text{Re}_x\text{Si}_2$ system in panel (c) are reversed relative to those of panels (a) and (b). The $T_0(x, P)$ data for the $\text{URu}_{2-x}\text{Re}_x\text{Si}_2$ system were taken from Ref. 18.

behavior in URu_2Si_2 .⁵⁹ The equivalence between $P_{ch}(x)$ and P is reflected in the consistent “additive” relationship $P_{ch}(x) + P_c \approx 1.5$ GPa, where the critical pressure P_c necessary to drive the HO \rightarrow LMAFM phase transition in $\text{URu}_{2-x}\text{Fe}_x\text{Si}_2$ decreases with increasing Fe concentration x . The relevance of pressure- and chemical-induced changes to the lattice and how they relate to hybridization between f - and d -electron states is discussed in more detail below.

The results presented here for the effect of increasing Os concentration x on the enhancement of HO in $\text{URu}_{2-x}\text{Os}_x\text{Si}_2$, as well as the reduction of the critical pressure P_c that induces the HO \rightarrow LMAFM transition, are remarkably similar to the phase behavior reported for Fe-substituted URu_2Si_2 .⁵⁹ However, the isoelectronic substitutions of Fe and Os have contrasting effects on the body-centered-tetragonal (bct) lattice. Substitution of smaller Fe ions at the Ru site leads to a contracted lattice and a *positive* chemical pressure $P_{ch}(x)$ in $\text{URu}_{2-x}\text{Fe}_x\text{Si}_2$, while substitution of larger Os ions at the Ru site leads to an expanded lattice and a *negative* chemical pressure $P_{ch}(x)$ in $\text{URu}_{2-x}\text{Os}_x\text{Si}_2$ (The effect of Os substitution on the lattice is given in Sec. VI.) This complicates the view of a reduction in the unit-cell volume through applied or chemical pressure as a necessary condition for the enhancement of HO in URu_2Si_2 .

Here we suggest an increase in the hybridization of the uranium $5f$ -electron states and transition metal d -electron states as the cause for the enhancement of HO toward the HO \rightarrow LMAFM phase transition in URu_2Si_2 . High-resolution angle-resolved photoemission spectroscopy (ARPES) and scanning-tunneling microscopy (STM) measurements show directly that the HO phase emerges from a paramagnetic (PM) Kondo phase that has clear signatures of hybridization (i.e., Kondo screening) between the localized $5f$ - and itinerant spd -electron states, with the onset of hybridization forming at a coherence temperature $T_{coh} \approx 70$ K.^{22,24–26,37} At lower temperatures close to the HO transition temperature T_0 , there is an increase in the $5f$ - d -electron hybridization leading to a Fermi surface instability as more U- $5f$ electrons dissolve into the FS.^{22,24–26,36,37,73,74} The degenerate crossing of hybridized $5f$ - d bands at the Fermi

energy E_F create density of states “hot spots” or instabilities at the Fermi surface in the PM phase.^{20,27} Hence, small perturbations to the electronic structure in the PM phase may lift the degeneracy and remove the FS instability leading to the opening of a “hybridization gap” over roughly 70% of the FS in the HO and LMAFM phases and a “re-hybridization” of the $5f$ - and d -electron states. Such a topological reconstruction of the FS is observed during the second-order symmetry-breaking transition (or Lifshitz transition) from the PM phase to the HO (or LMAFM) phase.

In this report, we suggest that when URu_2Si_2 is tuned with pressure or with either of the isoelectronic substitutions of Fe or Os at the Ru site, subtle changes occur to the $5f$ - d -electron hybridization near the Fermi level which favor the stability of the gapped FS of the HO (or LMAFM) phase over the instability of the FS in the Kondo-like PM phase. As a result, there is an observed increase in the transition temperature T_0 with increasing pressure P or substituent concentration x . This applies to the observed increase in T_N for the PM \rightarrow LMAFM phase transition, during which the FS undergoes a similar reconstruction and gapping. Inelastic neutron scattering experiments performed on single crystals from the $\text{URu}_{2-x}\text{Fe}_x\text{Si}_2$ system reveal similar interband correlations where enhanced local-itinerant electron hybridization also leads to the stability of the LMAFM phase.⁷⁵ Below, we address the manner in which each of the three perturbations (pressure, Fe substitution, and Os substitution) independently favors the hybridization of the U- $5f$ - and d -electron states. Hence, the additivity of x and P in enhancing HO and inducing the LMAFM phase in both the $\text{URu}_{2-x}\text{Fe}_x\text{Si}_2$ and $\text{URu}_{2-x}\text{Os}_x\text{Si}_2$ systems is also explained.

PRESSURE: Application of uniaxial and hydrostatic pressure both reveal that the pressure dependence of the HO transition temperature T_0 is anisotropic with respect to changes in the a and c lattice parameters of the tetragonal crystal. The a lattice parameter (or the shortest U-U separation in the basal plane of the tetragonal lattice) appears to be important in affecting the magnetic properties of URu_2Si_2 , as well as the transition to the LMAFM phase.^{65,71} Furthermore, it has been shown that it is not

possible to induce the HO→LMAFM phase transition with uniaxial stress along the c axis.⁷¹ Nor does the ratio of lattice parameters c/a appear to be important in governing the salient magnetic properties and phase behavior of URu_2Si_2 .⁷¹ These pressure-induced changes to the lattice are closely connected to spatial and energetic changes that may occur to the s -, p -, d -, and f -electronic orbitals. It is well known that the application of pressure reduces the interatomic distance within a crystal lattice leading to the delocalization and overlapping of electronic orbitals.^{76–79} As a consequence, applied pressure can lead to an increase in the hybridization between f - and d -electron states,^{80–82} which is important for the formation of the HO phase, and is now considered to be one of its defining characteristics.^{22,36,73} Here, we suggest that the pressure-induced enhancement of hybridization in URu_2Si_2 -based systems contributes to the instability at the FS that leads to the gapping of the FS and the second-order transition to the HO and LMAMF phases.

Fe-SUBSTITUTION: The remarkable agreement between $P_{ch}(x)$ and P , and their effect on the HO and LMAFM phases is not a surprise, considering that Fe substitution results in an almost entirely uniaxial contraction along the a parameter axis. Upon substitution of smaller Fe ions for Ru, it is suggested that the effective chemical pressure P_{ch} associated with the reduction in the interatomic spacing, favors increased overlap and hybridization of the U-5 f -electron states and d -electron states in much the same way that applied pressure P favors hybridization.^{57,59} Hence, the sum result for investigations of URu_2Si_2 under pressure and investigations of Fe substitution in $URu_{2-x}Fe_xSi_2$ suggest that a contracted lattice in the direction of the a axis is necessary for the enhancement of HO and a transition to LMAFM in URu_2Si_2 .^{57–59} In addition to the comparable effects of Fe substitution and pressure on the lattice, HO, and LMAFM, we discuss below the binding energy of the Fe-4 d electrons as a relevant factor for the increase in 5 f - and d -electron hybridization.

Os-SUBSTITUTION: In contrast, the effective “negative” chemical pressure associated with an expanded crystal lattice upon substitution of larger Os ions for Ru should not favor hybridization of the U-5 f - and d -electron states in $URu_{2-x}Os_xSi_2$. However, an increase in the hybridization may still occur if one considers one or both of the following: (1) The larger spatial extent of the 5 d -electron orbitals in osmium compared to that of the 4 d -electron orbitals in ruthenium where the change in the radius of the d -electron wave functions is 0.639 Å for Ru ions to 0.706 Å for Os ions.^{83,84} In the tight-binding approximation, the overlap for a pair of orbitals is dominated by an exponential term which decays on a length scale given by the inverse sum of the radii of the two electronic orbitals.^{85–87} The increase in the radius of the d -electron wave functions when an Os ion replaces a Ru ion is significant and would considerably effect the overlap of the d -electron wave functions and U-5 f -electron wave functions. (2) The stronger spin-orbit coupling that occurs in Os compared to that of Ru may

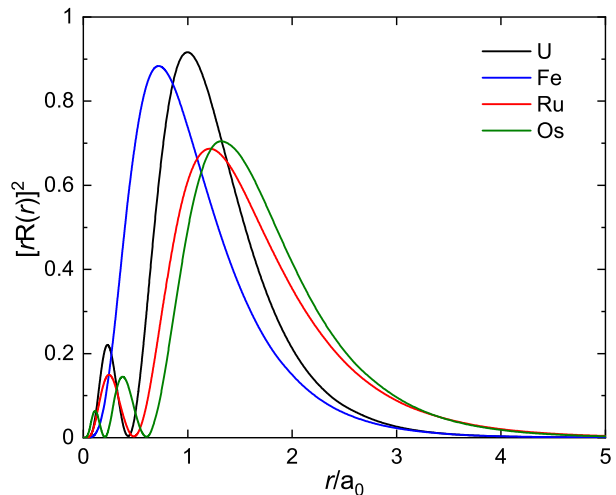


FIG. 8. (Color online) The radial probability distribution for the f - and d -electrons in U, Fe, Ru, and Os ions, expressed in atomic units.

lead to a broadening of the d -electron energy bands and an increase in the number of d electrons at the Fermi level.²⁷

Calculations of f - and d -electron hybridization in UM_2Si_2 with $M = (\text{Fe}, \text{Ru}, \text{and Os})$

In an effort to further understand the hybridization between the U 5 f -electron states and the transition metal d -electron states in the UM_2Si_2 series with $M = (\text{Fe}, \text{Ru}, \text{and Os})$, we performed tight-binding calculations of the overlap of the U-5 f -electron states and d -electron states of the Fe, Ru, and Os ions. Preliminary calculations of Hartree-Fock wave-functions were made for the U-5 f -electron states, the partially-filled d -electron shells of the transition metal ions Fe, Ru, and Os, as well as the 3 p -electron states of Si and 4 p -electron states of Ge. The radial probability distributions for the f - and d -electron states are displayed in Fig. 8. Relative to the 4 d -electron states of Ru, the 3 d -electron states of Fe are more localized, whereas the 5 d -electron states of Os are slightly more spatially extended.

Additionally, the Hartree-Fock binding energies E_{HF} for the f - and d -electron orbitals in U, Fe, Ru, and Os were calculated and are summarized in Table I. Note that there is a non-monotonic trend in the binding energy for the transition metal ions (Fe, Ru, and Os) moving down the column in the periodic table with $E_{HF} = 1.2157$, 0.80244, and 1.0095 ry for the Fe 3 d^6 , Ru 4 d^7 , and Os 5 d^6 states, respectively. The anomalous electronic configuration of atomic Ru sets its binding energy much lower than that of the d -electrons of Fe, Os. The binding energy of Ru is also much lower than that of the f -electrons of U where $E_{HF} = 1.2689$ ry for U 5 f^3 state.

Tight-binding energy matrix elements $t_{\alpha,\beta}(R)$ were calculated to determine the degree of overlap of the U-5 f -electron states with the Fe, Ru, and Os d -electron states

TABLE I. Hartree-Fock binding energies E_{HF} of f - and d -electron orbitals in U, Fe, Ru, and Os ions, where the energies are given in Rydbergs (Ry).

Element	Binding energy E_{HF} (Ry)
U $5f^3$	1.2689
Fe $3d^6$	1.2157
Ru $4d^7$	0.8024
Os $5d^6$	1.0096

for atomic sites separated by a distance R . Hybridization energies $\Delta_\alpha(R)$ were estimated from the matrix elements $t_{\alpha,\beta}(R)$ and from the calculated Hartree-Fock binding energies for the U, Fe, Ru, and Os ions in $\text{URu}_{2-x}\text{M}_x\text{Si}_2$ with $M = (\text{Fe}, \text{Os})$ according to the expression:

$$\Delta_\alpha(R) = \sum_\beta \frac{|t_{\beta,\alpha}(R)|^2}{E_{5f} - E_{d,\beta}}, \quad (1)$$

where $E_{5f} = 1.2689 \text{ ry}$ is the binding energy for the U $5f^3$ state and $E_{d,\beta} = 1.2157, 0.8024,$ and 1.0095 ry are the binding energies for the Fe $3d^6$, Ru $4d^7$, and Os $5d^6$ states, respectively (see Table I).

Table II contains the hybridization energies as a measure of the degree of hybridization between the U $5f$ -electron states and the d -electron states of Fe, Ru, and Os. The hybridization energies $\Delta_\alpha(R)$ are smallest for the hybridization of Ru d -electrons, which suggests a diminished hybridization for the d electrons of the Ru ions compared to those of the Fe and Os ions. Hybridization of the Os d -electron states with the U $5f$ -electron states is largest, being only slightly larger than that of the Fe d -electron states. This ordering of $\Delta_\alpha(R)$ for Fe, Ru, and Os is attributed to both the increasing spatial extent of the d -electron wave function down the column of the periodic table (Fig. 8) and also the non-monotonic variation in excitation energy (or binding energy). However, the non-monotonic variation in binding energy is the dominant effect, where the binding energy of the Ru d -electrons is much lower than that of the Fe and Os d -electrons and also the f -electrons of U (see Table I).

Similar trends in $4f$ - d -electron hybridization are reported for the heavy-Fermion and Kondo-like systems of CeFe_2Si_2 , CeRu_2Si_2 , and $\text{CeRu}_{2-x}\text{Os}_x\text{Si}_2$, where the strength of the hybridization of the Ce- $4f$ electrons and the s , p , and d conduction electrons can be characterized by the Kondo temperature T_K .⁸⁸ CeFe_2Si_2 has a large Kondo temperature $T_K \sim 103 \text{ K}$,⁸⁹ while the Kondo temperature for CeRu_2Si_2 is $T_K \sim 10$ to 25 K .^{88,90-92} As small amounts of Os are introduced into $\text{CeRu}_{2-x}\text{Os}_x\text{Si}_2$, the Kondo temperature increases to $T_K \sim 10^2 \text{ K}$ for $x = 0.1$.^{91,93} These changes in the

TABLE II. Hybridization energies of the α -th $5f$ -orbital with the β th d -orbital, where the energies are given in Rydbergs (Ry).

$\Delta_\alpha(R)$	Fe (Ry)	Ru (Ry)	Os (Ry)
$\Delta_{xyz}(R)$	0.081	0.034	0.097
$\Delta_{x(5x^2-3r^2)}(R)$	0.058	0.025	0.064
$\Delta_{y(5y^2-3r^2)}(R)$	0.050	0.021	0.055
$\Delta_{z(5z^2-3r^2)}(R)$	0.079	0.033	0.087
$\Delta_{x(y^2-z^2)}(R)$	0.039	0.018	0.047
$\Delta_{y(z^2-x^2)}(R)$	0.039	0.018	0.047
$\Delta_{z(x^2-y^2)}(R)$	0.067	0.028	0.084

hybridization of the Ce- $4f$ and s , p , and d electrons across the CeFe_2Si_2 , CeRu_2Si_2 , and $\text{CeRu}_{2-x}\text{Os}_x\text{Si}_2$ systems appear to be consistent with the changes in the $5f$ - d -electron hybridization in other reports⁹⁴ and with our calculations across the UM_2Si_2 series with $M = (\text{Fe}, \text{Ru}, \text{and Os})$.

Hence, the enhancement of the HO phase in $\text{URu}_{2-x}\text{Os}_x\text{Si}_2$ with increasing Os concentration x is consistent with the greater degree of d - and f -electron hybridization as calculated for the Os ions. Similar reasoning may also explain the enhancement of HO in the case of URu_2Si_2 under applied pressure P and the case of $\text{URu}_{2-x}\text{Fe}_x\text{Si}_2$ with increasing Fe concentration x . The reduction of the critical pressure P_c , and the cooperative effects of x and P observed in $\text{URu}_{2-x}\text{Os}_x\text{Si}_2$, may follow from the nature in which both the perturbations of x and P work together to foster hybridization: applied pressure favors delocalization of the U- $5f$ electrons and the substitution of Os ions for Ru extends the d electrons outward within the unit cell. Both of these effects together would favor overlap between the U- $5f$ - and d -electron wave functions in $\text{URu}_{2-x}\text{Os}_x\text{Si}_2$.

The increase in spin-orbit coupling may also help with hybridization of the U- $5f$ - and Os- $5d$ -electron states on account of the splitting of the d -electron band, which brings the orbitals closer together in energy and slightly enhances the hybridization between the two orbital levels with $j = l - 1$, where $l = 3$ for U and $l = 2$ for Os. The increase in hybridization between the U- $5f$ -electron states and the transition metal d -electron states, caused by the larger spin-orbit coupling of Os, is estimated to be limited and less than $\sim 2 \%$.⁸⁷

The persistence of the critical pressure at $P_c = 1.5 \text{ GPa}$, with increasing rhenium (Re) concentration in $\text{URu}_{2-x}\text{Re}_x\text{Si}_2$, suggests that any doping which suppresses HO may not be “additive” with pressure, and, as such, is not a perturbation that favors hybridization. Indeed, for small Re concentration ($x < 0.1$) in $\text{URu}_{2-x}\text{Re}_x\text{Si}_2$, the hidden order transition T_0 is rapidly reduced and for higher Re concentrations ($x > 0.1$),

the system enters a ferromagnetic state rather than the LMAFM phase.

Based on our hybridization calculations and previous reports of the trends in $5f$ - d -electron hybridization for the $3d$ -, $4d$ -, and $5d$ -electron orbitals, one might expect the same qualitative increase in hybridization (relative to the Ru $4d$ electrons) for the Re- $5d$ -electron states as observed for the Os- $5d$ -electron states. However, the trends in $5f$ - d -electron hybridization reported here for UM_2Si_2 ($M = \text{Fe, Ru, and Os}$) and elsewhere for CeM_2Si_2 ($M = \text{Fe, Ru, and Os}$)^{88,90–93} are for systems that are isoelectronic. For these systems, there is little or no variation across the series in the number of d -band electrons near the Fermi energy that are available for hybridization. The degree of f - d -electron hybridization is largely dependent on the density of states at the Fermi level such that any significant variation in the number of d electrons near E_F would have an effect on the hybridization.^{45,94} Furthermore, substitutions for Ru such as Rh and Re that are effectively electron (or hole) doping would shift the Fermi energy away from the degenerate crossing of the hybridized bands thereby stabilizing the FS in the paramagnetic phase. In addition, any doping resulting from non-isoelectronic substitutions might also change the underlying band structure and shape of the FS, which experimentally is shown to disrupt HO and replace it with an un-ordered state.^{95,96}

Hence, there are competing effects on hybridization in moving from Ru to Re, where any increase in hybridization owing to the spatially extended character of Re- $5d$ electrons is mitigated by the reduction in the number of d electrons available near E_F for hybridization and other deleterious effects to the FS. The d orbital electronic configuration is $5d^5$ for Re compared to $5d^6$ for Os. In the case of Re substitution, the decrease in the density of d -band electrons (or increase in hole concentration) may inhibit the $5f$ - d -electron hybridization that is observed to increase in the case of Os substitution. In addition, the degree of hybridization between U- $5f$ electrons and Re- $5d$ electrons depends not only on the hybridization matrix elements but also largely on the binding energy of the Re- $5d$ electrons (see Equation 1). Hence, a comparison of hybridization across systems that are not isoelectronic is more complicated and it is not unreasonable to assume that hybridization in the case of Re substitution would not increase as observed for the case of Os substitution. For systems in which the HO phase is suppressed with increasing substituent x , as in Re-substituted URu_2Si_2 , a determination of the hybridization between the U- $5f$ and Re- $5d$ electrons as a function of concentration x should be investigated further.

V. CONCLUSIONS

Early specific heat measurements of URu_2Si_2 in 1985 revealed an anomalous feature at $T_0 = 17.5$ K, reminiscent of a continuous mean-field type of phase transition.² The use of a simple model for the analysis of the specific

heat anomaly led to the notion of a partial gapping of the Fermi surface as the compound entered the hidden order (HO) phase, with the magnitude of the gap determined to be 11 meV.² This simple yet powerful experimental technique was one of the first “probes” into the structure or “reconstruction” of the Fermi surface during the HO phase transition in URu_2Si_2 . Over the last 20 years, advanced experimental techniques have yielded direct evidence and provided confirmation of the partial gapping of the Fermi surface, with gap values of ~ 10 meV. We now have a detailed picture of the electronic structure in proximity to the hidden order transition at T_0 , whereby the onset of hybridization of $5f$ and d electrons at 70 K leads to a degenerate crossing of $5f$ - d -hybridized bands at the Fermi level and ultimately to an instability, reconstruction, and partial gapping of the Fermi surface at 17.5 K.

Currently, applied pressure, and the substitution of Fe and Os ions for Ru, are the only known perturbations to URu_2Si_2 that result in an enhancement of HO and a subsequent first-order transition to the LMAFM phase. Here, we explain the enhancement of HO as the result of an increase in the hybridization of the uranium $5f$ - and transition metal (Fe, Ru, Os) d -electron states, which leads to a Fermi surface instability that favors the HO phase over the PM phase. This causes the increase in the PM→HO transition temperature T_0 .

The results from transport measurements for single crystals of $URu_{2-x}Os_xSi_2$ under pressure presented here are used to construct the $T_0(x, P)$ phase behavior. As the concentration of Os is increased, there is both an observed increase in T_0 and a reduction in the critical pressure P_c necessary to induce the transition to the LMAFM phase. This is consistent with previously reported effects of applied pressure and Fe substitution on HO and P_c in single crystals of $URu_{2-x}Fe_xSi_2$. However, the expansion of the lattice with increasing Os concentration is anomalous in comparison to the lattice contraction observed in URu_2Si_2 with increasing pressure and in $URu_{2-x}Fe_xSi_2$ with increasing Fe substitution.

Hence, the increase in the $5f$ - and d -electron hybridization appears to be dependent on various effects, both spatial and energetic. The contraction of the lattice with pressure or chemical pressure tends to favor both the overlap and hybridization of electronic orbitals, whereas the spatially extended d -electron orbitals (as with Os $5d$ electrons) can also lead to an increase in their hybridization with the “localized” $5f$ electrons. In this report, results of tight-binding calculations show that the degree of hybridization between the U $5f$ electrons with the transition metal d electrons is largely dependent on the difference in binding energy between the “localized” $5f$ electrons and d -band electrons. In general, it is noted that the trend in hybridization increases in moving away from the Ru $4d$ electrons to the Fe $3d$ and Os $5d$ electrons. This is true for other isoelectronic systems such as CeM_2Si_2 ($M = \text{Fe, Ru, and Os}$).

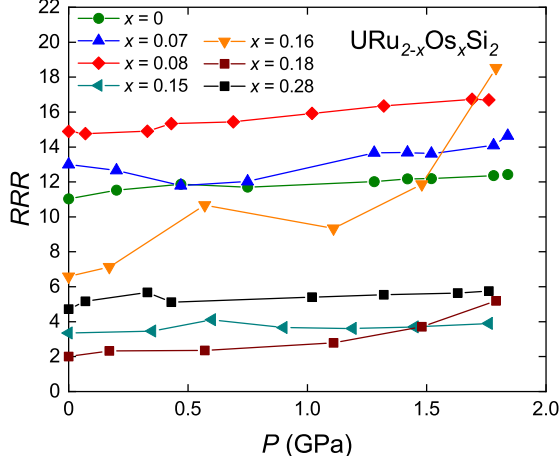


FIG. 9. (Color online) Values of the residual resistivity ratio (RRR) defined as $\rho(300K)/\rho(2K)$ as a function of pressure P for single crystal samples with $x = 0, 0.07, 0.08, 0.15, 0.16, 0.18, 0.28$.

VI. APPENDIX: SAMPLE QUALITY

There are some differences among the single crystal samples in the temperature dependence of the electrical resistivity at ambient pressure at the PM \rightarrow HO/LMAFM transition (see Fig. 1). The features at the transition temperature T_0 are relatively sharp for the $x = 0, 0.07, 0.08,$ and 0.16 samples, whereas for $x = 0.15, 0.18,$ and 0.28 samples, the transition at T_0 is broadened. These differences in the $\rho(T)$ behavior warrant some clarification and additional comments regarding the quality of the single crystal samples. We note that there will be some unavoidable and intrinsic broadening of the transition for larger concentrations of osmium. This type of broadening is also seen in the polycrystal data for Os concentrations larger than $x = 0.2$ previously reported in Ref. 61 and also in other work reported in Ref. 62, in which the feature in the $\rho(T)$ data at T_0 is nearly non-existent for the $x = 0.1$ sample. The broadening of the transition at T_0 may be attributed to inhomogeneity that arises when single crystals are grown out of melts in a tetra-arc furnace by the Czochralski method. As larger concentrations of Os are introduced into the melt, there is a larger chance of the occurrence of inhomogeneity across the sample.

The broadening of the transition at T_0 also occurs with increasing pressure. From the $\rho(T)$ data displayed in Fig. 3(a), the degree of broadening appears to be monotonic with increasing pressure. This type of pressure-induced broadening of the PM \rightarrow HO transition has been previously reported for polycrystalline URu_2Si_2 (see Fig. 1 in Ref. 6), where the broadening of the $\rho(T)$ feature at T_0 may be associated with “different states of strain within the polycrystalline sample”.⁶ Similar broadening of the HO transition occurred in single crystals of URu_2Si_2 ($x = 0$) under applied hydrostatic pressure (see Ref. 18). Broadening of the transition at T_0 is also seen in single crystal samples of $\text{URu}_{2-x}\text{Fe}_x\text{Si}_2$ as a function of increasing Fe concentration x (see Ref. 59). Hence,

the broadening of the T_0 transition observed in the single crystal samples of $\text{URu}_{2-x}\text{Os}_x\text{Si}_2$ with $x = 0.18$ and 0.28 (see Fig. 1) is not to be unexpected. However, the broadening in the $x = 0.15$ sample is somewhat anomalous and needs some clarification.

As a measure of sample quality, we deter-

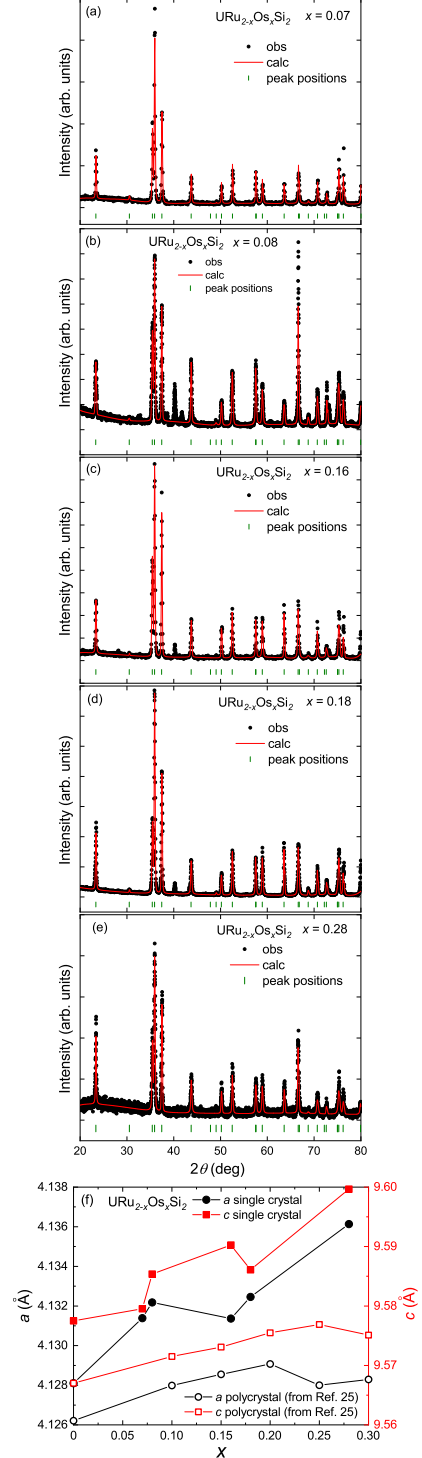


FIG. 10. (Color online) (a)–(e) X-ray diffraction patterns for single crystal samples of $\text{URu}_{2-x}\text{Os}_x\text{Si}_2$ with Os concentrations $x = 0.07, 0.08, 0.16, 0.18, 0.28$. The red line is the Rietveld refinement fit to the data in black. (f) Lattice parameters a and c versus osmium concentration x .

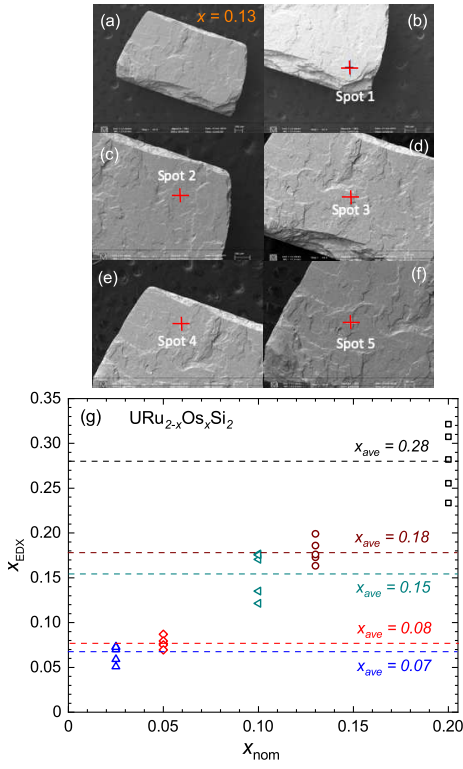


FIG. 11. (Color online) Results of EDX measurements for single crystal samples of $URu_{2-x}Os_xSi_2$ with nominal concentrations of $x_{nom} = 0.025, 0.05, 0.10, 0.13,$ and 0.20 . (a) Image of the single crystal sample with $x_{nom} = 0.13$. (b)–(f) An illustrative example of a set EDX measurements at five different spots over the surface of the $x_{nom} = 0.13$ sample. (g) Plot of the five osmium concentrations x_{EDX} from EDX measurements versus x_{nom} for each sample. Horizontal dashed lines are located at the average Os concentration x_{ave} of the five x_{EDX} values and are taken as the actual Os concentration $x_{act} = x$ for each sample.

mined the residual resistivity ratio (RRR), defined as $\rho(300K)/\rho(2K)$, for each of the single crystal samples. Values of RRR as a function of pressure P are displayed in Fig. 9 for single crystal samples with Os concentration $x = 0, 0.07, 0.08, 0.15, 0.16, 0.18, 0.28$. Note that for all samples, RRR increases with P , which is likely due to the improvement in the contact resistance between the leads and the sample as pressure is increased. At ambient pressure, the values of RRR are larger than 10 for those samples with lower Os concentration ($x = 0, 0.07, 0.08$). In comparison, significantly lower values of RRR = 3.3, 2, and 4.7 for the $x = 0.15, 0.18,$ and 0.28 samples suggest more inhomogeneity or the presence of impurity-induced electron scattering, which is likely to cause some broadening of the $\rho(T)$ feature at the transition temperature T_0 .

X-ray diffraction (XRD) patterns for single crystal samples of $URu_{2-x}Os_xSi_2$ with Os concentrations $x = 0.07, 0.08, 0.16, 0.18, 0.28$ are shown in Fig. 10(a)–(e). The black circles represent the data, the red line represents the fit results from Rietveld refinement to the data, and the green ticks indicate peak positions for the

URu_2Si_2 crystal. The peaks in the data at $2\theta = 40^\circ$ for $x = 0.08$ in panel (b), $x = 0.16$ in panel (c), and $x = 0.18$ in panel (d) are Os impurities. The results from the fits of the Rietveld refinement to the XRD data were used to determine the lattice constants a and c for single crystal samples of $URu_{2-x}Os_xSi_2$ with $x = 0.07, 0.08, 0.16, 0.18, 0.28$. The lattice constants a and c for single crystals (filled symbols) as well as for polycrystalline samples (open symbols) are plotted in Fig. 10(f) as a function of osmium concentration up to $x = 0.3$. (The polycrystal data was taken from Ref. 61.) For the single crystal samples, both lattice constants a and c are shown to increase by approximately 0.2% as Os concentration x is increased in $URu_{2-x}Os_xSi_2$. For the single crystal samples, there is some degree of scatter in the expansion of both a and c between $x = 0.08$ and 0.18 , which may be related to the presence of Os impurity peaks detected in the XRD patterns for the $x = 0.08, 0.16,$ and 0.18 samples (see Fig. 10).

Single crystal samples of $URu_{2-x}Os_xSi_2$ at nominal concentrations of $x_{nom} = 0.025, 0.05, 0.10, 0.13,$ and 0.20 were measured for elemental composition using energy-dispersive X-ray spectroscopy (EDX). For each of these samples, EDX measurements were made at five different spots across the surface of the sample. As a representative example, an image of a sample from the $x = 0.13$ single crystal is shown in Fig. 11(a) and the locations of the five different EDX measurement spots for this sample are shown in the images displayed in Fig. 11(b)–(f). The results of the EDX measurements for these samples are shown in Fig. 11(g), where the Os concentrations (x_{EDX}) determined from the five different EDX measurements on each sample are plotted (open symbols) versus the nominal Os concentration (x_{nom}). The horizontal dashed lines represent the average Os concentration x_{ave} of the five different EDX measurements for each sample, where x_{ave} is taken to be the actual osmium concentration x_{act} for these single crystal samples. Based on the EDX measurements, the single crystal samples of $URu_{2-x}Os_xSi_2$ with nominal concentrations of $x_{nom} = 0.025, 0.05, 0.10, 0.13,$ and 0.20 were determined to have actual concentrations of $x_{act} = 0.07, 0.08, 0.15, 0.18,$ and 0.28 , respectively. The error in the Os concentration for each sample is taken as the standard deviation of the five x_{EDX} values and is represented by the error bars in the T_0 – x phase diagram shown in Fig. 2. Note that for samples with larger concentrations of Os x , there is an increase in the error of x suggesting that the inhomogeneity across the sample increases as x increases. For the sample that was unavailable for EDX measurement, with nominal Os concentration of $x = 0.16$, the error in the Os concentration was taken as the average of the error for the samples with comparable Os concentration, namely $x = 0.15, 0.18,$ and 0.28 .

ACKNOWLEDGEMENTS

Research at the University of California, San Diego was supported by the US Department of Energy (DOE), Office of Basic Energy Sciences, Division of Materials Sciences and Engineering, under Grant DE-FG02-04ER46105 (materials synthesis and characterization), the US National Science Foundation (NSF) under Grant

DMR 1810310 (low-temperature measurements), and the National Nuclear Security Administration under the Stewardship Science Academic Alliance Program through the US DOE under Grant DE-NA0002909 (high-pressure measurements). Research at the National High Magnetic Field Laboratory (NHMFL) was supported by NSF Cooperative Agreement DMR-1157490, the State of Florida, and the DOE.

-
- ¹ T. T. M. Palstra, A. A. Menovsky, J. van den Berg, A. J. Dirkmaat, P. H. Kes, G. J. Nieuwenhuys, and J. A. Mydosh, “Superconducting and Magnetic Transitions in the Heavy-Fermion System URu₂Si₂,” *Phys. Rev. Lett.* **55**, 2727 (1985).
- ² M. B. Maple, J. W. Chen, Y. Dalichaouch, T. Kohara, C. Rossel, M. S. Torikachvili, M. W. McElfresh, and J. D. Thompson, “Partially Gapped Fermi Surface in the Heavy-Electron Superconductor URu₂Si₂,” *Phys. Rev. Lett.* **56**, 185 (1986).
- ³ W. Schlabitz, J. Baumann, B. Pollit, U. Rauchschwalbe, H. M. Mayer, U. Ahlheim, and C. D. Bredl, “Superconductivity and Magnetic Order in a Strongly Interacting Fermi-System: URu₂Si₂,” *Z. Phys. B - Condensed Matter* **62**, 171 (1986).
- ⁴ C. Broholm, J. K. Kjems, W. J. L. Buyers, P. Matthews, T. T. M. Palstra, A. A. Menovsky, and J. A. Mydosh, “Magnetic Excitations and Ordering in the Heavy-Electron Superconductor URu₂Si₂,” *Phys. Rev. Lett.* **58**, 1467–1470 (1987).
- ⁵ J. Schoenes, C. Schönerberger, J. J. M. Franse, and A. A. Menovsky, “Hall-effect and resistivity study of the heavy-fermion system URu₂Si₂,” *Phys. Rev. B* **35**, 5375–5378 (1987).
- ⁶ M. W. McElfresh, J. D. Thompson, J. O. Willis, M. B. Maple, T. Kohara, and M. S. Torikachvili, “Effect of pressure on competing electronic correlations in the heavy-electron system URu₂Si₂,” *Phys. Rev. B* **35**, 43–47 (1987).
- ⁷ A. LeR Dawson, W. R. Datars, J. D. Garrett, and F. S. Razavi, “Electrical transport in uru₂si₂,” *Journal of Physics: Condensed Matter* **1**, 6817 (1989).
- ⁸ T. E. Mason and W. J. L. Buyers, “Spin excitations and the electronic specific heat of URu₂Si₂,” *Phys. Rev. B* **43**, 11471 (1991).
- ⁹ C. Broholm, H. Lin, P. T. Matthews, T. E. Mason, W. J. L. Buyers, M. F. Collins, A. A. Menovsky, J. A. Mydosh, and J. K. Kjems, “Magnetic excitations in the heavy-fermion superconductor URu₂Si₂,” *Phys. Rev. B* **43**, 12809 (1991).
- ¹⁰ P. Santini and G. Amoretti, “Crystal Field Model of the Magnetic Properties of URu₂Si₂,” *Phys. Rev. Lett.* **73**, 1027 (1994).
- ¹¹ W. J. L. Buyers, Z. Tun, T. Petersen, T. E. Mason, J.-G. Lussier, B. D. Gaulin, and A. A. Menovsky, “Spin wave collapse and incommensurate fluctuations in URu₂Si₂,” *Physica B: Condensed Matter* **199-200**, 95 (1994).
- ¹² R. Escudero, F. Morales, and P. Lejay, “Temperature dependence of the antiferromagnetic state in URu₂Si₂ by point-contact spectroscopy,” *Phys. Rev. B* **49**, 15271 (1994).
- ¹³ H. Amitsuka, M. Sato, N. Metoki, M. Yokoyama, K. Kuwahara, T. Sakakibara, H. Morimoto, S. Kawarazaki, Y. Miyako, and J. A. Mydosh, “Effect of Pressure on Tiny Antiferromagnetic Moment in the Heavy-Electron Compound URu₂Si₂,” *Phys. Rev. Lett.* **83**, 5114–5117 (1999).
- ¹⁴ P. Chandra, P. Coleman, J. A. Mydosh, and V. Tripathi, “Hidden orbital order in the heavy fermion metal URu₂Si₂,” *Nature* **417**, 831 (2002).
- ¹⁵ F. Bourdarot, B. Fåk, K. Habicht, and K. Prokeš, “Inflection Point in the Magnetic Field Dependence of the Ordered Moment of URu₂Si₂ Observed by Neutron Scattering in Fields up to 17 T,” *Phys. Rev. Lett.* **90**, 067203 (2003).
- ¹⁶ C. R. Wiebe, G. M. Luke, Z. Yamani, A. A. Menovsky, and W. J. L. Buyers, “Search for hidden orbital currents and observation of an activated ring of magnetic scattering in the heavy fermion superconductor URu₂Si₂,” *Phys. Rev. B* **69**, 132418 (2004).
- ¹⁷ K. Behnia, R. Bel, Y. Kasahara, Y. Nakajima, H. Jin, H. Aubin, K. Izawa, Y. Matsuda, J. Flouquet, Y. Haga, Y. Ōnuki, and P. Lejay, “Thermal Transport in the Hidden-Order State of URu₂Si₂,” *Phys. Rev. Lett.* **94**, 156405 (2005).
- ¹⁸ J. R. Jeffries, N. P. Butch, B. T. Yukich, and M. B. Maple, “Competing Ordered Phases in URu₂Si₂: Hydrostatic Pressure and Rhenium Substitution,” *Phys. Rev. Lett.* **99**, 217207 (2007).
- ¹⁹ C. R. Wiebe, J. A. Janik, G. J. MacDougall, G. M. Luke, J. D. Garrett, H. D. Zhou, Y.-J. Jo, L. Balicas, Y. Qiu, J. R. D. Copley, Z. Yamani, and W. J. L. Buyers, “Gapped itinerant spin excitations account for missing entropy in the hidden-order state of URu₂Si₂,” *Nat. Phys* **3**, 96 (2007).
- ²⁰ S. Elgazzar, J. Ruzs, M. Amft, P. M. Oppeneer, and J. A. Mydosh, “Hidden order in URu₂Si₂ originates from Fermi surface gapping induced by dynamic symmetry breaking,” *Nat. Mat* **8**, 337 (2009).
- ²¹ J. A. Janik, H. D. Zhou, Y. J. Jo, L. Balicas, G. J. MacDougall, G. M. Luke, J. D. Garrett, K. J. McClellan, E. D. Bauer, J. L. Sarrao, Y. Qiu, J. R. D. Copley, Z. Yamani, W. J. L. Buyers, and C. R. Wiebe, “Itinerant spin excitations near the hidden order transition in URu₂Si₂,” *Journal of Physics: Condensed Matter* **21**, 192202 (2009).
- ²² Andrés F. Santander-Syro, Markus Klein, Florin L. Boariu, Andreas Nuber, Pascal Lejay, and Friedrich Reinert, “Fermi-surface instability at the ‘hidden-order’ transition of URu₂Si₂,” *Nat. Phys.* **5**, 637 (2009).
- ²³ K. Haule and G. Kotliar, “Complex Landau-Ginzburg theory of the hidden order in URu₂Si₂,” *EPL (Europhysics Letters)* **89**, 57006 (2010).
- ²⁴ Rikiya Yoshida, Yoshiaki Nakamura, Masaki Fukui, Yoshinori Haga, Etsuji Yamamoto, Yoshichika Ōnuki, Mario Okawa, Shik Shin, Masaaki Hirai, Yuji Muraoka, and Takayoshi Yokoya, “Signature of hidden order and evidence for periodicity modification in URu₂Si₂,” *Phys. Rev. B* **82**,

- 205108 (2010).
- 25 A. R. Schmidt, M. H. Hamidian, P. Wahl, F. Meier, A. V. Balatsky, J. D. Garrett, T. J. Williams, G. M. Luke, and J. C. Davis, "Imaging the Fano lattice to 'hidden order' transition in URu_2Si_2 ," *Nature* **465**, 570 (2010).
 - 26 Pegor Aynajian, Eduardo H. da Silva Neto, Colin V. Parker, Yingkai Huang, Abhay Pasupathy, John Mydosh, and Ali Yazdani, "Visualizing the formation of the Kondo lattice and the hidden order in URu_2Si_2 ," *Proc. Nat. Acad. Sci.* **107**, 10383 (2010).
 - 27 P. M. Oppeneer, J. Ruzs, S. Elgazzar, M.-T. Suzuki, T. Durakiewicz, and J. A. Mydosh, "Electronic structure theory of the hidden-order material URu_2Si_2 ," *Phys. Rev. B* **82**, 205103 (2010).
 - 28 P. M. Oppeneer, S. Elgazzar, J. Ruzs, Q. Feng, T. Durakiewicz, and J. A. Mydosh, "Spin and orbital hybridization at specifically nested Fermi surfaces in URu_2Si_2 ," *Phys. Rev. B* **84**, 241102 (2011).
 - 29 Ikuto Kawasaki, Shin-ichi Fujimori, Yukiharu Takeda, Tetsuo Okane, Akira Yasui, Yuji Saitoh, Hiroshi Yamagami, Yoshinori Haga, Etsuji Yamamoto, and Yoshichika Onuki, "Band structure and Fermi surface of URu_2Si_2 studied by soft x-ray angle-resolved photoemission spectroscopy," *Phys. Rev. B* **83**, 235121 (2011).
 - 30 Georgi L. Dakovski, Yinwan Li, Steve M. Gilbertson, George Rodriguez, Alexander V. Balatsky, Jian-Xin Zhu, Krzysztof Gofryk, Eric D. Bauer, Paul H. Tobash, Antoinette Taylor, John L. Sarrao, Peter M. Oppeneer, Peter S. Riseborough, John A. Mydosh, and Tomasz Durakiewicz, "Anomalous femtosecond quasiparticle dynamics of hidden order state in URu_2Si_2 ," *Phys. Rev. B* **84**, 161103 (2011).
 - 31 Yonatan Dubi and Alexander V. Balatsky, "Hybridization Wave as the "Hidden Order" in URu_2Si_2 ," *Phys. Rev. Lett.* **106**, 086401 (2011).
 - 32 J. T. Haraldsen, Y. Dubi, N. J. Curro, and A. V. Balatsky, "Hidden-order pseudogap in URu_2Si_2 ," *Phys. Rev. B* **84**, 214410 (2011).
 - 33 C. Pépin, M. R. Norman, S. Burdin, and A. Ferraz, "Modulated Spin Liquid: A New Paradigm for URu_2Si_2 ," *Phys. Rev. Lett.* **106**, 106601 (2011).
 - 34 Peter S. Riseborough, B. Coqblin, and S. G. Magalhães, "Phase transition arising from the underscreened Anderson lattice model: A candidate concept for explaining hidden order in URu_2Si_2 ," *Phys. Rev. B* **85**, 165116 (2012).
 - 35 J. A. Mydosh and P. M. Oppeneer, "*Colloquium* : Hidden order, superconductivity, and magnetism: The unsolved case of URu_2Si_2 ," *Rev. Mod. Phys.* **83**, 1301–1322 (2011).
 - 36 J.-Q. Meng, P. M. Oppeneer, J. A. Mydosh, P. S. Riseborough, K. Gofryk, J. J. Joyce, E. D. Bauer, Y. Li, and T. Durakiewicz, "Imaging the Three-Dimensional Fermi-Surface Pairing near the Hidden-Order Transition in URu_2Si_2 Using Angle-Resolved Photoemission Spectroscopy," *Phys. Rev. Lett.* **111**, 127002 (2013).
 - 37 F. L. Boariu, C. Bareille, H. Schwab, A. Nuber, P. Lejay, T. Durakiewicz, F. Reinert, and A. F. Santander-Syro, "Momentum-Resolved Evolution of the Kondo Lattice into "Hidden Order" in URu_2Si_2 ," *Phys. Rev. Lett.* **110**, 156404 (2013).
 - 38 C. Bareille, F. L. Boariu, H. Schwab, P. Lejay, F. Reinert, and A. F. Santander-Syro, "Momentum-resolved hidden-order gap reveals symmetry breaking and origin of entropy loss in URu_2Si_2 ," *Nat. Commun.* **5**, 637 (2009).
 - 39 J. A. Mydosh and P. M. Oppeneer, "Hidden order behaviour in URu_2Si_2 (A critical review of the status of hidden order in 2014)," *Philos. Mag.* **94**, 3642–3662 (2014).
 - 40 Nicholas P. Butch, Michael E. Manley, Jason R. Jeffries, Marc Janoschek, Kevin Huang, M. B. Maple, Ayman H. Said, Bogdan M. Leu, and Jeffrey W. Lynn, "Symmetry and correlations underlying hidden order in URu_2Si_2 ," *Phys. Rev. B* **91**, 035128 (2015).
 - 41 Sheng Ran, Christian T. Wolowiec, Inho Jeon, Naveen Pouse, Noravee Kanchanavatee, Benjamin D. White, Kevin Huang, Dinesh Martien, Tyler DaPron, David Snow, Mark Williamsen, Stefano Spagna, Peter S. Riseborough, and M. Brian Maple, "Phase diagram and thermal expansion measurements on the system $\text{URu}_{2-x}\text{Fe}_x\text{Si}_2$," *Proc. Nat. Acad. Sci.* **113**, 13348 (2016).
 - 42 H.-H. Kung, S. Ran, N. Kanchanavatee, V. Krapivin, A. Lee, J. A. Mydosh, K. Haule, M. B. Maple, and G. Blumberg, "Analogy Between the "Hidden Order" and the Orbital Antiferromagnetism in $\text{URu}_{2-x}\text{Fe}_x\text{Si}_2$," *Phys. Rev. Lett.* **117**, 227601 (2016).
 - 43 Sheng Ran, Inho Jeon, Naveen Pouse, Alexander J. Breindel, Noravee Kanchanavatee, Kevin Huang, Andrew Gallagher, Kuan-Wen Chen, David Graf, Ryan E. Baumbach, John Singleton, and M. Brian Maple, "Phase diagram of $\text{URu}_{2-x}\text{Fe}_x\text{Si}_2$ in high magnetic fields," *Proc. Nat. Acad. Sci.* **114**, 9826–9831 (2017).
 - 44 Y. Dalichaouch, M. B. Maple, M. S. Torikachvili, and A. L. Giorgi, "Ferromagnetic instability in the heavy-electron compound URu_2Si_2 doped with Re or Tc," *Phys. Rev. B* **39**, 2423 (1989).
 - 45 Y. Dalichaouch, M. B. Maple, J. W. Chen, T. Kohara, C. Rossel, M. S. Torikachvili, and A. L. Giorgi, "Effect of transition-metal substitutions on competing electronic transitions in the heavy-electron compound URu_2Si_2 ," *Phys. Rev. B* **41**, 1829 (1990).
 - 46 Y. Dalichaouch, M. B. Maple, R. P. Guertin, M.V. Kuric, M. S. Torikachvili, and A. L. Giorgi, "Ferromagnetism and heavy electron behavior in $\text{URu}_{2-x}\text{M}_x\text{Si}_2$ ($\text{M} = \text{Re}, \text{Tc}$ and Mn)," *Physica B: Condensed Matter* **163**, 113 (1990).
 - 47 N. P. Butch and M. B. Maple, "The suppression of hidden order and the onset of ferromagnetism in URu_2Si_2 via Re substitution," *Journal of Physics: Condensed Matter* **22**, 164204 (2010).
 - 48 Makoto Yokoyama, Hiroshi Amitsuka, Seiichiro Itoh, Ikuto Kawasaki, Kenichi Tenya, and Hideki Yoshizawa, "Neutron Scattering Study on Competition between Hidden Order and Antiferromagnetism in $\text{U}(\text{Ru}_{1-x}\text{Rh}_x)_2\text{Si}_2$ ($x \leq 0.05$)," *J. Phys. Soc. Japan* **73**, 545 (2004).
 - 49 A. Lopez de la Torre, P. Visani, Y. Dalichaouch, B. W. Lee, and M. B. Maple, "Th-doped URu_2Si_2 : influence of Kondo holes on coexisting superconductivity and magnetism," *Physica B: Condensed Matter* **179**, 208 (1992).
 - 50 J. G. Park and B. R. Coles, "Studies of alloying effects on $\text{URu}_2(\text{Si},\text{X})_2$; $\text{X} = \text{Al}$ or Ge ," *Journal of Physics: Condensed Matter* **6**, 1425 (1994).
 - 51 S. Zwirner, J. C. Waerenborgh, F. Wastin, J. Rebizant, J. C. Spirlet, W. Potzel, and G. M. Kalvius, "Anisotropic magnetic coupling in $\text{Np}_x\text{U}_{1-x}\text{PdAl}_3$, $\text{Np}_x\text{U}_{1-x}\text{Ru}_2\text{Si}_2$," *Physica B: Condensed Matter* **230-232**, 80 (1997), *Proc. Intl. Conf. Strongly Correlated Electron Systems*.
 - 52 A. Gallagher, K. W. Chen, C. M. Moir, S. K. Cary, F. Kametani, N. Kikugawa, D. Graf, T. E. Albrecht-Schmitt, S. C. Riggs, A. Shekhter, and R. E. Baumbach, "Unfolding the physics of URu_2Si_2 through silicon to phosphorus substitution," *Nature Comm.* **7**, 10712 (2016).
 - 53 N. P. Butch, J. R. Jeffries, S. Chi, J. B. Leão, J. W. Lynn, and M. B. Maple, "Antiferromagnetic critical pressure in

- URu₂Si₂ under hydrostatic conditions,” *Phys. Rev. B* **82**, 060408 (2010).
- ⁵⁴ J. R. Jeffries, N. P. Butch, B. T. Yukich, and M. B. Maple, “The evolution of the ordered states of single-crystal URu₂Si₂ under pressure,” *J. of Phys.: Condens. Matter* **20**, 095225 (2008).
- ⁵⁵ F. Bourdarot, B. Fåk, V. P. Mineev, M. E. Zhitomirsky, N. Kernavanois, S. Raymond, F. Lapiere, P. Lejay, and J. Flouquet, “Pressure dependence of magnetic transitions in URu₂Si₂,” *Physica B* **350**, E179 – E181 (2004), Proceedings of the Third European Conference on Neutron Scattering.
- ⁵⁶ H. Amitsuka, K. Matsuda, I. Kawasaki, K. Tenya, M. Yokoyama, C. Sekine, N. Tateiwa, T.C. Kobayashi, S. Kawarazaki, and H. Yoshizawa, “Pressure-temperature phase diagram of the heavy-electron superconductor URu₂Si₂,” *J. of Magn. and Magn. Mater.* **310**, 214 – 220 (2007).
- ⁵⁷ N. Kanchanavatee, M. Janoschek, R. E. Baumbach, J. J. Hamlin, D. A. Zocco, K. Huang, and M. B. Maple, “Twofold enhancement of the hidden-order/large-moment antiferromagnetic phase boundary in the URu_{2-x}Fe_xSi₂ system,” *Phys. Rev. B* **84**, 245122 (2011).
- ⁵⁸ P. Das, N. Kanchanavatee, J. S. Helton, K. Huang, R. E. Baumbach, E. D. Bauer, B. D. White, V. W. Burnett, M. B. Maple, J. W. Lynn, and M. Janoschek, “Chemical pressure tuning of URu₂Si₂ via isoelectronic substitution of Ru with Fe,” *Phys. Rev. B* **91**, 085122 (2015).
- ⁵⁹ C. T. Wolowiec, N. Kanchanavatee, K. Huang, S. Ran, and M. B. Maple, “Evolution of critical pressure with increasing Fe substitution in the heavy-fermion system URu_{2-x}Fe_xSi₂,” *Phys. Rev. B* **94**, 085145 (2016).
- ⁶⁰ M. N. Wilson, T. J. Williams, Y.-P. Cai, A. M. Hallas, T. Medina, T. J. Munsie, S. C. Cheung, B. A. Frandsen, L. Liu, Y. J. Uemura, and G. M. Luke, “Antiferromagnetism and hidden order in isoelectronic doping of URu₂Si₂,” *Phys. Rev. B* **93**, 064402 (2016).
- ⁶¹ N. Kanchanavatee, B. D. White, V. W. Burnett, and M. B. Maple, “Enhancement of the hidden order/large moment antiferromagnetic transition temperature in the URu_{2-x}Os_xSi₂ system,” *Philos. Mag.* **94**, 3681 (2014).
- ⁶² Jesse S. Hall, M. R. Movassagh, M. N. Wilson, G. M. Luke, N. Kanchanavatee, K. Huang, M. Janoschek, M. B. Maple, and T. Timusk, “Electrodynamics of the antiferromagnetic phase in URu₂Si₂,” *Phys. Rev. B* **92**, 195111 (2015).
- ⁶³ J.D Denlinger, G.-H Gweon, J.W Allen, C.G Olson, M.B Maple, J.L Sarrao, P.E Armstrong, Z Fisk, and H Yamagami, “Comparative study of the electronic structure of xRu₂Si₂: probing the Anderson lattice,” *Journal of Electron Spectroscopy and Related Phenomena* **117-118**, 347 (2001), strongly correlated systems.
- ⁶⁴ Brian H. Toby and Robert B. Von Dreele, “*GSAS-II*: the genesis of a modern open-source all purpose crystallography software package,” *Journal of Applied Crystallography* **46**, 544 (2013).
- ⁶⁵ S. Kambe, D. Aoki, B. Salce, F. Bourdarot, D. Braithwaite, J. Flouquet, and J.-P. Brison, “Thermal expansion under uniaxial pressure in URu₂Si₂,” *Phys. Rev. B* **87**, 115123 (2013).
- ⁶⁶ M. B. Fontes, J. C. Trochez, B. Giordanengo, S. L. Bud’ko, D. R. Sanchez, E. M. Baggio-Saitovitch, and M. A. Continentino, “Electron-magnon interaction in RNiBC (*R* = Er, Ho, Dy, Tb, and Gd) series of compounds based on magnetoresistance measurements,” *Phys. Rev. B* **60**, 6781–6789 (1999).
- ⁶⁷ K. Matsuda, Y. Kohori, T. Kohara, K. Kuwahara, and H. Amitsuka, “Spatially Inhomogeneous Development of Antiferromagnetism in URu₂Si₂: Evidence from ²⁹Si NMR under Pressure,” *Phys. Rev. Lett.* **87**, 087203 (2001).
- ⁶⁸ M. Nakashima, H. Ohkuni, Y. Inada, R. Settai, Y. Haga, E. Yamamoto, and Y. Onuki, “The de Haas-van Alphen effect in URu₂Si₂ under pressure,” *J. of Phys.: Condens. Matter* **15**, S2011 (2003).
- ⁶⁹ A. Villaume, F. Bourdarot, E. Hassinger, S. Raymond, V. Taufour, D. Aoki, and J. Flouquet, “Signature of hidden order in heavy fermion superconductor URu₂Si₂: Resonance at the wave vector Q₀ = (1, 0, 0),” *Phys. Rev. B* **78**, 012504 (2008).
- ⁷⁰ P. G. Niklowitz, C. Pfeleiderer, T. Keller, M. Vojta, Y.-K. Huang, and J. A. Mydosh, “Parasitic Small-Moment Antiferromagnetism and Nonlinear Coupling of Hidden Order and Antiferromagnetism in URu₂Si₂ Observed by Larmor Diffraction,” *Phys. Rev. Lett.* **104**, 106406 (2010).
- ⁷¹ Frederic Bourdarot, Nicolas Martin, Stephane Raymond, Louis-Pierre Regnault, Dai Aoki, Valentin Taufour, and Jacques Flouquet, “Magnetic properties of uru₂si₂ under uniaxial stress by neutron scattering,” *Phys. Rev. B* **84**, 184430 (2011).
- ⁷² T. J. Williams, H. Barath, Z. Yamani, J. A. Rodriguez-Riviera, J. B. Leão, J. D. Garrett, G. M. Luke, W. J. L. Buyers, and C. Broholm, “Gapped excitations in the high-pressure antiferromagnetic phase of URu₂Si₂,” *Phys. Rev. B* **95**, 195171 (2017).
- ⁷³ S. Chatterjee, J. Trinckauf, T. Hänke, D. E. Shai, J. W. Harter, T. J. Williams, G. M. Luke, K. M. Shen, and J. Geck, “Formation of the Coherent Heavy Fermion Liquid at the Hidden Order Transition in URu₂Si₂,” *Phys. Rev. Lett.* **110**, 186401 (2013).
- ⁷⁴ E. Frantzeskakis, J. Dai, T. C. Rödel, M. Guttler, C. Bareille, S. Ran, N. Kanchanavatee, K. Huang, N. Pouse, C. T. Wolowiec, E. D. L. Rienks, P. Lejay, T. Durakiewicz, F. Fortuna, Maple M. B., and Andrés F. Santander-Syro, “From hidden-order to antiferromagnetism: electronic structure reconstruction in Fe-doped URu₂Si₂,” Submitted.
- ⁷⁵ Nicholas P. Butch, Sheng Ran, Inho Jeon, Noravee Kanchanavatee, Kevin Huang, Alexander Breindel, M. Brian Maple, Ryan L. Stillwell, Yang Zhao, Leland Harriger, and Jeffrey W. Lynn, “Distinct magnetic spectra in the hidden order and antiferromagnetic phases in URu_{2-x}Fe_xSi₂,” *Phys. Rev. B* **94**, 201102 (2016).
- ⁷⁶ H.G. Drickamer, “The Effect of High Pressure on the Electronic Structure of Solids,” *Solid State Physics* **17**, 1 – 133 (1965).
- ⁷⁷ H. G. Drickamer and C. W. Frank, *Electronic Transitions and the High Pressure Chemistry and Physics of Solids*, ed., Studies in Chemical Physics (Springer Netherlands, Netherlands, 1973).
- ⁷⁸ James S. Schilling, “Pressure as a parameter in the study of dilute magnetic alloys,” *Adv. Phys.* **28**, 657 (1979).
- ⁷⁹ James S. Schilling, “Some Recent Results in Magnetism under High Pressure,” in *Physics of Solids under High Pressure*, edited by James S. Schilling and Robert S. Shelton (North-Holland Publishing Company, Amsterdam, 1981) pp. 345–356.
- ⁸⁰ M. B. Maple, J. Wittig, and K. S. Kim, “Pressure-Induced Magnetic-Nonmagnetic Transition of Ce Impurities in La,” *Phys. Rev. Lett.* **23**, 1375 (1969).
- ⁸¹ K. S. Kim and M. B. Maple, “Kondo Effect in La_{1-x}Ce_x Alloys under Pressure,” *Phys. Rev. B* **2**, 4696 (1970).

- ⁸² M. B. Maple, "Superconductivity - a probe of the magnetic state of local moments in metals," *Applied physics* **9**, 179 (1976).
- ⁸³ J. B. Mann, "SCF Hartree-Fock results for elements with two open shells and the elements francium to nobelium," *Atomic Data and Nuclear Data Tables* **12**, 1 (1973).
- ⁸⁴ A. D. McLean and R. S. McLean, "Roothaan-Hartree-Fock atomic wave functions Slater basis-set expansions for $Z = 55-92$," *Atomic Data and Nuclear Data Tables* **26**, 197 (1981).
- ⁸⁵ D. A. Papaconstantopoulos and M. J. Mehl, "The Slater-Koster tight-binding method: a computationally efficient and accurate approach," *J. Phys.: Condens. Matter* **15**, R413 (2003).
- ⁸⁶ J. Durgavich, S. Sayed, and D. Papaconstantopoulos, "Extension of the NRL tight-binding method to include f orbitals and applications in Th, Ac, La and Yb," *Comp. Mater. Sci.* **112**, 395 (2016).
- ⁸⁷ D. A. Papaconstantopoulos, *Handbook of the Band Structure of Elemental Solids*, 2nd ed. (Springer US, New York, NY, 2015).
- ⁸⁸ L. P. Regnault, W. A. C. Erkelens, J. Rossat-Mignod, P. Lejay, and J. Flouquet, "Neutron scattering study of the heavy-fermion compound CeRu_2Si_2 ," *Phys. Rev. B* **38**, 4481 (1988).
- ⁸⁹ M. Koterlyn, I. Shcherba, R. Yasnitskii, and G. Koterlyn, "Peculiarities of the intermediate valence state of Ce in CeM_2Si_2 ($M=\text{Fe}, \text{Co}, \text{Ni}$) compounds," *Journal of Alloys and Compounds* **442**, 176 (2007), proceedings of the 15th International Conference on Solid Compounds of Transition Elements.
- ⁹⁰ M.J. Besnus, J.P. Kappler, P. Lehmann, and A. Meyer, "Low temperature heat capacity, magnetization, resistivity of CeRu_2Si_2 , with Y or La substitution," *Solid State Communications* **55**, 779 (1985).
- ⁹¹ A Umarji, Godart Claude, L Gupta, and R Vijayaraghavan, "Spin fluctuation effects in substituted CeRu_2Si_2 and YbPd_2Si_2 alloys," *Pramana* **27**, 321 (1986).
- ⁹² Yoshio Kitaoka, Koh-ichi Ueda, Kenji Fujiwara, Hironobu Arimoto, Haruhisa Iida, and Kunisuke Asayama, "NMR Investigation of Superconductivity and Kondo-Coherency in CeCu_2Si_2 ," *Journal of the Physical Society of Japan* **55**, 723 (1986).
- ⁹³ C. Godart, A. M. Umarji, L. C. Gupta, and R. Vijayaraghavan, "Magnetism and spin fluctuation effects in heavy-fermion CeRu_2Si_2 induced by partial substitution of Ru and Si," *Phys. Rev. B* **34**, 7733 (1986).
- ⁹⁴ Andrea Amorese, Martin Sundermann, Brett Leedahl, Andrea Marino, Daisuke Takegami, Hlynur Gretarsson, Andrei Hloskovsky, Christoph Schlüter, Maurits W. Haverkort, Yingkai Huang, Maria Szlawaska, Dariusz Kaczorowski, Sheng Ran, M. Brian Maple, Eric D. Bauer, Andreas Leithe-Jasper, Peter Thalmeier, Liu Hao Tjeng, and Andrea Severing, "Dual nature of 5f electrons in the isostructural UM_2Si_2 family: from antiferro- to Pauli paramagnetism via hidden order," arXiv: 2004.13419 (2020), arXiv:2004.13419 [cond-mat.str-el].
- ⁹⁵ Y. S. Oh, Kee Hoon Kim, P. A. Sharma, N. Harrison, H. Amitsuka, and J. A. Mydosh, "Interplay between Fermi Surface Topology and Ordering in URu_2Si_2 Revealed through Abrupt Hall Coefficient Changes in Strong Magnetic Fields," *Phys. Rev. Lett.* **98**, 016401 (2007).
- ⁹⁶ Y. J. Jo, L. Balicas, C. Capan, K. Behnia, P. Lejay, J. Flouquet, J. A. Mydosh, and P. Schlottmann, "Field-Induced Fermi Surface Reconstruction and Adiabatic Continuity between Antiferromagnetism and the Hidden-Order State in URu_2Si_2 ," *Phys. Rev. Lett.* **98**, 166404 (2007).